NeuroImage 217 (2020) 116908

Contents lists available at ScienceDirect

NeuroImage

journal homepage: www.elsevier.com/locate/neuroimage

Dissociable neural correlates of stimulation intensity and detection in somatosensation

Norman Forschack [a,b,*], Till Nierhaus [b,c], Matthias M. Müller [a], Arno Villringer [b,d,**]

[a] Experimental Psychology and Methods, University of Leipzig, 04109, Leipzig, Germany
[b] Max Planck Institute for Human Cognitive and Brain Sciences, 04103, Leipzig, Germany
[c] Neurocomputation and Neuroimaging Unit, Department of Education and Psychology, Freie Universität Berlin, 14195, Berlin, Germany
[d] MindBrainBody Institute at Berlin School of Mind and Brain, Charité and Humboldt-Universität zu Berlin, 10117, Berlin, Germany

ARTICLE INFO

Keywords:
Somatosensory detection
Event-related potentials
Pre-stimulus rolandic oscillations
Subthreshold electrical stimulation
Regularized logistic regression
Baysian null-hypotheses testing

ABSTRACT

Somatosensory stimulation intensity and behavioral detection are positively related, and both correlate with neural responses. However, it is still controversial as to what extent stimulus intensity and early somatosensory evoked potentials (SEP) predict detection and how these parameters interact with pre-stimulus brain oscillatory states, which also influence sensory processing. Here we investigated how early SEP components encode stimulation intensity, how pre-stimulus alpha- and beta-band amplitudes interact with SEPs, and which neural markers predict stimulus detection. To this end, we randomly presented electrical finger nerve stimulation with various intensities distributed along the individual psychometric response function (including catch trials) while recording the EEG. Participants reported stimulus presence on a trial-by-trial basis (one-alternative-forced-choice). For the lowest (imperceptible) intensities, participants showed zero (behavioral) sensitivity despite measurable early cortical processing reflected by the P50 component. The P50 amplitude scaled with increasing stimulation intensities but was not predictive of stimulus detection. Instead, detection was associated with the later negative N150 component, as well as with pre-stimulus lowered somatosensory alpha- and increased frontal beta-band amplitudes. Our results give evidence for a serial representation of stimulus intensity and detection, as reflected by the P50 and N150 amplitude, respectively. Furthermore, stimulus detection seems to depend on the current brain state, rendering upcoming stimulation being reportable or not.

Significance statement

Investigating neural processes of perception without awareness might reveal prerequisites of the neural correlates of consciousness. In the current EEG study, we employed imperceptible stimulation, for which participants did not experience any sign of perceptual awareness. In addition, we presented stimuli of varying stimulation intensity above the detection threshold to dissociate the neural correlates of stimulus detection and intensity. We found that the amplitude of an early event-related component —the P50— (1) is measurable after imperceptible stimulation, (2) is driven by stimulation intensity, but (3) does not predict upcoming stimulus detection when we analyzed detected and rejected stimuli of the same intensity. The successive N150 best explains behavioral performance and might depend on endogenous content (re) activation that is signified by frontal beta band amplitudes. Lower central alpha and higher frontal beta amplitudes support stimulus detection and seem necessary to trigger perceptual awareness.

1. Introduction

Investigating neural processes of perception without awareness may disclose neural phenomena that preclude conscious perception (Baumgarten et al., 2017; Blankenburg et al., 2003; Forschack et al., 2017; Merikle and Daneman, 1998; Nierhaus et al., 2015). Additionally, it may reveal markers that are necessary but, apparently, not sufficient for conscious perception and, therefore could reflect prerequisites of the neural correlates of consciousness (NCC, Aru et al., 2012). Research dedicated to the identification of electrophysiological predictors of

* Corresponding author. Experimental Psychology and Methods, University of Leipzig, Institute of Psychology, Neumarkt 9 - 19, Entrance D 04109, Leipzig, Germany 04109, Leipzig, Germany, Stephanstraße 1a, 04103, Leipzig, Germany.
** Corresponding author. Max Planck Institute for Human Cognitive and Brain Sciences, Department of Neurology, Stephanstraße 1a, 04103, Leipzig, Germany.
E-mail addresses: norman.forschack@uni-leipzig.de (N. Forschack), villringer@cbs.mpg.de (A. Villringer).

https://doi.org/10.1016/j.neuroimage.2020.116908
Received 26 July 2019; Received in revised form 30 April 2020; Accepted 3 May 2020
Available online 6 May 2020

somatosensory detection agrees on the involvement of mid-range somatosensory event-related potentials (SEPs) occurring after stimulus presentation, however, differs on the involvement of earlier SEP components, specifically regarding the strength of the P50 (Auksztulewicz and Blankenburg, 2013; Auksztulewicz et al., 2012; Frey et al., 2016; Palva et al., 2005). These studies typically applied stimulation intensities individually tuned to exert detection on 50% of the trials, often called "near-threshold" (NTH) stimulation. Whereas Auksztulewicz and colleagues (2012, 2013) found the most prominent effect of perceptual awareness to occur locally as a negative potential over contralateral somatosensory areas roughly peaking 140 ms after stimulus presentation, both Frey et al. (2016) and Palva et al. (2005) reported global (i.e., across-area) awareness differences even before 60 ms.

A different line of research investigated electrophysiological responses to stimulation below the absolute detection threshold (ADTH, Forschack et al., 2017; Klostermann et al., 2009; Libet et al., 1967; Nierhaus et al., 2015; Ray et al., 1999). Detection rates to these imperceptible stimuli are comparable to false alarm rates to catch trials, i.e., trials without any stimulation. The above-mentioned studies reported, that stimulation below ADTH (i.e., subthreshold) evokes a P50 but no further components. While these results agree with the notion that the mere presence of the P50 is not sufficient for stimulus detection, a proper test to the hypothesis that its amplitude or latency might play a role in stimulus detection at different intensities along the individual psychometric function, is hitherto absent. On the contrary, data from a somatosensory extinction patient, i.e., a patient showing detection performance loss due to unilateral brain damage, indicated that attenuation rather than elimination of somatosensory P50 in the damaged hemisphere might cause tactile extinction (Eimer et al., 2002). Furthermore, previous studies never proved the imperceptibility below ADTH intensity by bias-free sensitivity measures of stimulus detection (Baumgarten et al., 2017; Blankenburg et al., 2003; Iliopoulos et al., 2014; Klostermann et al., 2009; Libet et al., 1967; Nierhaus et al., 2015; Ray et al., 1999; Shevrin and Fritzler, 1968; Taskin et al., 2008) or assumed chance performance by non-significant d-prime values (Bernat et al., 2001a, 2001b; Ferrè et al., 2016; Forschack et al., 2017; Shevrin, 2001). While the former studies cannot control for individual response tendencies (e.g., a general reluctance to report stimulus detection or the contrary), the latter do not provide a decisive test for imperceptibility. Thus, the current study set out to quantify the contribution of somatosensory electrophysiological response strength in stimulus detection by explicitly manipulating stimulation intensities along the individual psychometric function of healthy human volunteers. Specifically, we tested (1) whether stimulation below ADTH intensity can be shown to be reliably imperceptible using Bayesian statistics, (2) whether the amplitude of the P50 component only correlates with stimulus intensity or (3), for a sufficiently high intensity, would also reflect detection. Furthermore, pre-stimulus oscillatory amplitudes both in the alpha- and beta band have been observed to influence tactile perception (Anderson and Ding, 2011; Baumgarten et al., 2016; Craddock et al., 2017; Forschack et al., 2017; Linkenkaer-Hansen et al., 2004; Schubert et al., 2008; Weisz et al., 2014; Zhang and Ding, 2009). Thus, we explored (4) the contribution of pre-stimulus oscillatory amplitudes in the alpha- as well as the beta-band on stimulus detection and their possible modulation of SEP components.

2. Materials and methods

2.1. Participants

The local ethics committee at the medical faculty of the University of Leipzig approved the study. Before participation, all volunteers underwent a comprehensive neurological examination that screened for a history of neurological or psychiatric diseases or any medication. Forty healthy volunteers participated (age range 20–35 yrs, mean 27.2 ± 3.8 yrs S.D.; 21 females); all were right-handed (laterality score according to the Oldfield questionnaire: mean 92.4 ± 12.8 S.D., over a range of −100 (entirely left-handed) to 100 (entirely right-handed), Oldfield, 1971). Data of four participants were discarded due to defective (n = 2) or artifactual (n = 2) EEG recordings, thus in total 36 datasets were analyzed.

Based on our previous findings, we expected the smallest SEP component following 50 ms (P50) after subthreshold stimulation. One goal of the study was to show that despite zero behavioral sensitivity to subthreshold stimulation, the latter nevertheless evokes the P50. Thus, we calculated the required sample size for an effect size of 0.52 (Cohen's *d* based on the average P50-SEP potential contralateral to an attended finger receiving subthreshold stimulation, see Forschack et al., 2017) with a power (1-β error probability) of 0.85 and an α error probability of 0.05 using G*Power (Faul et al., 2007). The required minimum sample size is 35, so we considered 36 subjects to be of an adequate size to study the P50 potential modulations for stimuli of different intensities including the range below absolute detection threshold (see below).

2.2. Experimental procedures

2.2.1. Somatosensory stimulation

Electrical finger nerve stimulation was applied by constant-current stimulators (DS7, Digitimer, Welwyn Garden City, Hertfordshire, United Kingdom). Single current pulses (quantified in milliampere, mA) are adjusted to have a monophasic square wave shape of 200 μs consistent with previous studies (Blankenburg et al., 2003; Forschack et al., 2017; Iliopoulos et al., 2014; Nierhaus et al., 2015; Taskin et al., 2008). A custom-built interface to the DS7 allowed automatic adjustment of stimulation magnitudes in steps of 0.1 mA. Custom scripts running in the stimulation software "Presentation" (Neurobehavioral Systems, San Francisco, U.S.A.) triggered electrical pulses. Stimulator output was delivered through a pair of steel wire ring electrodes attached to the middle (anode) and the proximal (cathode) phalanx of the left index finger.

2.2.2. Threshold assessment and task design

The experimental session comprised ten blocks (duration about 7 min per block) each starting with the threshold assessment. Every block contained 134 trials with or without stimulation (i.e., 1340 trials overall). Preceding each block, a trained experimenter manually assessed the individual ADTH with the same two-step procedure as in our previous studies (Forschack et al., 2017; Nierhaus et al., 2015). Briefly, this procedure applies one trial of ascending stimulation intensities and asks the participant to indicate a conscious sensation as soon as one emerges. In the second step, comprising 30–60 trials (about 5 min), the experimenter presented current intensities (with a resolution of 0.1 mA) around this roughly estimated detection threshold to find the lowest current intensity at which participants report a sensation in a yes/no-detection-task scheme. Importantly, the experimenter also applied trials without any stimulation ("catch trials"), in about 20% of all trials to control for individual response tendencies. ADTH is then the smallest stimulus magnitude for which participant's detection rate ("hit rate") exceeds the false alarm rate of the catch trials.

Furthermore, suprathreshold intensity (STH) was individually adjusted to be the first that is perceived throughout all trials during a stimulus detection run. This assessment applied five different intensities above ADTH and separated by 0.1 mA (five repetitions for each and five catch trials) that remained constant for 2 min (method of constants). If no STH intensity could be identified, stimulation intensities were increased by 0.2 mA, and further stimulus detection runs were conducted until STH criterion was reached. Finally, we defined six different intensities relative to the estimated ADTH and STH, which were then applied during the experimental blocks: two different subthreshold intensities (subTH-30%, subTH-15%, i.e., 70% and 85% of ADTH intensity, 420 trials each), the ADTH intensity (100 trials), two near-threshold intensities (NTH33%, NTH66%: 100 trials each), whose current intensities equally divided the distance (in mA) between ADTH and STH, as well as the STH intensity

(100 trials). Note that the number of subthreshold trials is more than four times higher than for the other intensities to increase the signal-to-noise ratio for the subthreshold P50.

Participants were informed that on every trial they would either receive a detectable, undetectable stimulus or no stimulation at all, but that they always have to decide whether a stimulus was there or not (forced-choice Yes/No detection (1AFC) task). Trial duration was fixed to 3000 ms and started with gaze fixation at a centrally presented cross on a monitor screen in front of the participants. In a period of 1200 ms up to 2000 ms after fixation onset, either a single current pulse with one of the six individually defined intensities was presented pseudo-randomly (1240 trials) or no stimulation was applied (100 catch trials). Upon switch from fixation cross to question mark (i.e., at 3000 ms after fixation onset), participants indicated detection of a stimulus by pressing the left ("detected") or the right button ("nothing detected") of a response box with the index or middle finger of the right hand, respectively. The question mark either disappeared after 1000 ms or as soon as participants pressed either button; then a new trial started.

2.2.3. EEG acquisition

During 10 stimulation blocks each lasting roughly 7 min, we recorded EEG continuously from 62 channels (61 scalp electrodes plus 1 electrode recording the VEOG below the right eye; actiCap, BrainAmp, Brain Products, Munich, Germany) attached according to the 10-10 system (Oostenveld and Praamstra, 2001), referenced to midfrontal electrode (FCz) and grounded to an electrode placed at the sternum. Impedances were kept $\leq$5 kΩ for all channels, sampling frequency 2.5 kHz, analog filter low-cutoff at 0.016 Hz and high cutoff at 1000 Hz.

Data analysis was performed offline using the R framework (R Core Team, 2014, RRID:SCR_001905) together with the RStudio front end (RStudio Team, 2012, RRID:SCR_000432) and MATLAB (MathWorks, RRID:SCR_001622) applying custom-built scripts and toolbox algorithms from EEGLAB (Delorme and Makeig, 2004, RRID:SCR_007292).

2.3. Behavioral analysis

Behavioral data were aggregated into hit- and false alarm rates (HR, FAR), i.e., the probability of responding "yes" when a stimulus was presented or responding "no" when there was no stimulation, respectively. Both measures are affected by the observer's perceptual sensitivity to a stimulation intensity and an individual response tendency towards reporting or not reporting a signal independent of whether one is presented or not (Green and Swets, 1966; Kingdom and Prins, 2009; Macmillan and Creelman, 2004; Swets, 1961, 1964). Therefore, perceptual sensitivity is calculated as *d*-prime (Macmillan and Creelman, 2004):

$$d' = z(HR) - z(FAR)$$

where the function z(x) is the inverse-normal transformation and converts hit and false alarm rates ranging from 0 to 1 to *z* scores having zero mean and a standard deviation of one. We used the "log-linear" method to account for extreme portions of the data (i.e., hit and false alarm rates of zero or one) and pooled trials across blocks for the calculation of *d*-prime values to minimize the method's biasing effect with respect to the true value.

With a *d*-prime value of zero, observers are not able to discriminate a stimulus at all, i.e., HR = FAR. A stimulus that exerts zero perceptual sensitivity, therefore, satisfies the condition of escaping conscious perception, because objective performance is at chance. For two reasons this situation, though, is hard to meet: 1. *d*-prime values of exactly zero cannot be achieved with limited and noisy data sets. 2. Testing the null hypothesis (NH), as it is required for proving chance performance, cannot be accomplished by classical test theoretic procedures. Frequentist statistics are designed to reject the null and to be sensitive for the alternative hypothesis (Rouder et al., 2009). If the NH is true, p-values are equally likely and may take on any value between 0 and 1 (Rouder et al., 2009). Bayes factors, instead, evaluate the probability of the NH, i.e., chance performance, against the probability of the alternative given the observed data, i.e., the odds ratio. An odds ratio of two means that the NH is two times more likely than the alternative. We adopt the common convention by Lee and Wagenmakers (2013) that classifies odds ratios of more than three as moderate and more than ten as strong evidence in favor of the hypothesis in the numerator.

Bayes Factors are influenced by the distribution of prior probabilities across different effect sizes. For an objective statistical proof of chance performance exerted by subthreshold stimulation, we chose priors with minimal assumptions about the range of effect sizes under the alternative. Therefore, we applied the so-called JZS prior—a combination of the Cauchy distribution on effect size and the Jeffreys prior on variance (Rouder et al., 2009)—as it neither defines a specific effect size nor a single value for its variance under the alternative hypothesis. The JZS prior might be scaled when smaller or larger effect sizes are expected a priori (ibid.). However, here we consider a range of scales, *r*, to relax strong expectations about the effect size.

Stimulation conditions that did not exert a significant effect in *d*-prime in a one-sample *t*-test against zero were submitted to a Bayes factor analysis incorporating the JZS-prior (scaling factor $r = \sqrt{2}/2 \approx 0.707$) to evaluate the evidence for the NH against the AH. This approach was implemented in R using the "BayesFactor"-package by Richard D. Morey. To estimate the effect of JZS prior scaling on the odds ratio, Bayes factor analysis was repeated for different *r* ranging from 0.1 to 1.5 putting relatively more weight on small to large effect sizes, respectively. The resulting Bayes Factors have been visualized using the statistics software JASP (JASP Team, 2018, RRID:SCR_015823). In the current study, there were fewer catch trials (by a factor of four) than trials with subthreshold stimulation intensities. Therefore, false alarm rates to the former were expected to show more variance above zero compared to hit rates to the latter. The *z*-transformation used for the calculation of *d*' values would further amplify this difference especially for response rates below 0.1 that might result in biased *d*' values below zero. We, therefore, implemented Bayes factor analysis as a paired two-sample test of hit rates to subthreshold stimulation versus false alarm rates to catch trials. Note that this procedure is comparable to testing *d*' values against zero but results in a more conservative estimate of the true (null) effect. To check whether observers are still able to classify stimulation below ADTH, *d'* values for both subthreshold stimulation intensities were compared via paired Bayes factor test. Any bias to the *d'* values – as described above – would affect both conditions and, thus, is negligible.

2.4. EEG data analysis

2.4.1. Preprocessing

First, we applied a low-pass finite impulse response filter (high cut-off: 150 Hz, transition bandwidth: 50 Hz) before downsampling the continuous EEG to 500 Hz.

Next, we ran the standardized early-stage EEG processing pipeline (PREP, Bigdely-Shamlo et al., 2015) on the downsampled data. This algorithm first removes 50 Hz line noise by subtracting a frequency domain regression model of the best-fitting deterministic sinusoid in the range of 48–52 Hz estimated by a sliding window multi-taper approach (Mullen, 2012). Then, the algorithm re-referenced the continuous data to a robust average reference signal derived by iteratively detecting and interpolating noisy channels (interpolation based on all but the VEOG electrode). Next, individual datasets underwent independent component analysis (ICA, adaptive mixture of independent component analyzers (AMICA), Palmer et al., 2011) both to remove sources of ocular and muscle artifacts as well as signals of other non-neural origin (Chaumon et al., 2015; Delorme et al., 2012; Li et al., 2006). Prior to ICA, datasets were prepared by applying the following procedures: training datasets for ICA were high-pass filtered with 1 Hz, all blocks were concatenated, and contiguous epochs of 1 s were extracted, corrected for average epoch potential, screened for non-stereotypical artifacts and rejected if

contaminated. Then, an initial ICA was performed after which artifactual epochs were identified in ICA space using improbable data estimation on single and across all components and removed semi-automatically (function "pop_jointprob", threshold limit for single channels: 4.5 SD, threshold limit for all channels: 2.5 SD, Delorme et al., 2007). The resulting datasets were submitted to a second ICA (again using AMICA algorithm). We visually inspected the new set of components and identified artifactual components based on various features of IC topographies and time courses calculated by SASICA (Semi-Automated Selection of Independent Components of the electroencephalogram for Artifact correction, Chaumon et al., 2015). Specifically, we rejected components showing correlations with VEOG channel higher than 0.6 or horizontal EOG (bipolarized potential of channel "FT7" and "FT8") higher than 0.4, blink or eye movement typical topographies and IC source activity, abnormal frequency spectrum, i.e., high frequency or line noise, focal topographies as indicative of non-neural origin. Only the unmixing and sphering matrices of artifact-free components were forward-projected to high-pass filtered *continuous* datasets for the subsequent analysis steps (function "pop_firws" Widmann et al., 2015; low cut-off of 0.1 Hz, Kaiser window, maximum passband deviation: 0.001 and transition bandwidth: 0.2 Hz, resulting filter order of 9056, i.e., a filter length of 9057 data points estimated by the *pop_firwsord* function). On average, 25 (5 SD) out of 57 (2 SD) components were rejected. The median rank of rejected components, when sorted by descending mean projected variance variance is 33 (i.e., artifactual components contain less variance of the data as compared to the retained components).

Data for SEP analysis was further low-pass filtered by a Kaiser windowed sinc finite impulse response filter with a high cut-off of 41 Hz (high cut-off maximum pass-band deviation: 0.0001 and transition bandwidth: 10.25 Hz, resulting filter order of 246). Proper epochs were cut from the continuous channel signals ranging from −1200 to 3600 ms relative to stimulus onset (t = 0), from which the individual epoch mean was subtracted. Epochs exceeding the joint logarithmic probability of 4.5 or 2.5 SD within or across all independent components (i.e., including artifactual components), respectively, were discarded after manually reviewing the alleged artifactual epochs (Delorme et al., 2007). Additionally, trials that contained behavioral response within −800 to 800 ms relative to stimulus onset, as well as reaction times smaller than 150 ms or higher than 1100 ms, have been excluded. Finally, the following average number of trials per stimulation condition remained for the primary analyses: 374 (21 S.D.) subTH-30%, 371 (22 S.D.) subTH-15%, 90 (5 S.D.) ADTH, 90 (5 S.D.) NTH33%, 88 (6 S.D.) NTH-66%, 87 (6 S.D.) STH and 89 (5 S.D.) for catch trials. Linear detrending was applied to these remaining trials over a time range of −0.6–1.2 s to remove any sustained potential drifts.

2.4.2. Amplitude and latency extraction of SEP components and their statistical analysis concerning stimulation intensity

From our previous studies, we had strong a-priori hypotheses concerning the presence of the P50 and N150 and, therefore, we focused our analyses on these components in the signal of the contralateral central "C4" electrode (Nierhaus et al., 2015; Forschack et al., 2017). A topographical test of the post-stimulus period (0–300 ms) averaged across all stimulation conditions compared to a pre-stimulus baseline ranging from −100 to 0 ms to stimulus onset was conducted to estimate the sensibility of this selection. For multiple comparisons correction (i.e., time and electrodes), we applied threshold-free cluster enhancement (TFCE) with a cluster threshold of $p = 0.05$ (cluster size exponent E = 0.5, statistical intensity exponent H = 2, Mensen and Khatami, 2013; Smith and Nichols, 2009). For this, topographical isocontour voltage maps of P50 and N150 component peaks are represented.

Baseline corrected (−100 to 0 ms) P50 and N150 SEP peak amplitudes and latencies of the stimulation condition averages were extracted for each participant as neural markers indicative of perceptual changes along the psychometric response function. To this end, we ran a peak and latency detection algorithm within time windows of interest: 32–76 ms for the P50 peak latency and 128 to 172 for the N150 peak latency, based on the SEP from the tfce permutation test (see above). Average maximal component amplitudes and latency values were plotted together with respective within-subject confidence intervals (Cousineau et al., 2005; Loftus and Masson, 1994; Morey, 2008). Pairwise two-tailed t-tests ($p < 0.05$) were calculated for each stimulation condition pair and corrected for multiple comparisons using false discovery rate (fdr, q = 0.05, Benjamini and Hochberg, 1995; Genovese et al., 2002). Additionally, we performed one post-hoc *t*-test on the time-course of the averaged subTH SEP against baseline to reveal potential further components following P50 (fdr-corrected).

The six different stimulation intensities were fixed within each block. To test whether detected and rejected trials are comparable with regard to stimulation intensities across blocks, we calculated average stimulation current for each participant and stimulation condition, separately for all trials classified being detected and rejected, respectively. Resulting values were subjected to a paired one-sample *t*-test.

2.4.3. Rolandic rhythms

To discern Rolandic rhythms from occipital alpha activity, we used an a priori selection of central contralateral electrodes ("C2", "C4", "C6", "CP2", "CP4", and "CP6"), based on the electrodes found to be predictive for somatosensory masking (Schubert et al., 2008). For this, we convolved every trial of each stimulation condition with complex Morlet wavelets tuned to include 5.5 cycles of frequencies ranging from 4 to 42 Hz. Frequency bands of interest were defined based on the results by Schubert et al. (2008). However, neighboring alpha and beta bands in Schubert et al. (2008) were slightly overlapping. We, therefore, redefined frequency bands of interest to be more distinct. I.e., the alpha band ranged from 9 to 14 Hz and the beta band from 20 to 30 Hz. Wavelet parameters resulted in the following frequency and time smoothing: 3.85 Hz at full-width-half-maximum (FWHM) and 114.5 ms (+/− FWHM) at 9 Hz; 5.99 Hz (FWHM) and 73.6 ms (+/− FWHM) at 14 Hz; 8.56 Hz (FWHM) and 51.5 ms at 20 Hz (+/− FWHM). The pre-stimulus window that was going to be tested for its relation to stimulus detection, we chose it to be as close as possible to stimulus presentation but without smearing into the post-stimulus window; i.e., this window should not include latencies higher than −114.5 ms relative to stimulus onset for the 9 Hz frequency response. This procedure avoids that power from the stimulus related SEPs leak into the pre-stimulus window. This window we defined from −400 to −150 ms relative to stimulus onset for all analyzed frequencies, which is congruent with the time window in which Schubert et al. (2008) found the frequency band effects. Statistical analysis was performed by testing the pre-stimulus time-frequency-band-of-interest response of the central contralateral and frontal electrode cluster for detected versus rejected stimulation (NTH66% and STH only) with cluster-based two-tailed paired *t*-tests (*p*-level was set to 0.01 and corrected for multiple comparisons by tfce, Mensen and Khatami, 2013).

2.4.4. Prediction of stimulus detection by SEP amplitude and latency and rolandic alpha and beta amplitude

To identify neural markers generally predictive for stimulus detection, we calculated SEPs separately for detected and rejected finger pulses at the same central contralateral electrode cluster (see above) and averaged these across NTH66% and STH stimulation intensities. Specifically, we tested whether P50 and N150 latency and amplitude are predictive for behavioral classification. To this end, we applied binomial regularized logistic regression together with six-fold cross-validation (James et al., 2015) to select the essential neural markers for stimulus detection. This procedure selects the best model out of a set of regressors. Regularization was achieved by adding the so-called lasso penalty—or ℓ_1 norm—to the standard maximum-likelihood model coefficient optimization. The influence of this penalty was controlled by the tuning parameter λ ranging from 0 to 100, where zero puts no penalty on the coefficients of the full model and corresponds to standard generalized linear modeling (glm). With increasing λ, regressor coefficients are

shrunk towards zero depending on their predictive value for behavioral response classification; thus, the higher λ, the simpler the model. For model selection, we chose the model that shows the smallest cross-validation error (CVE) across all λ. Model fit was further evaluated by statistically evaluating classification accuracy with one-sided binomial tests against 0.5 (i.e., 50% accuracy for random choices).

To assess a probable influence of pre-stimulus Rolandic rhythms on neural markers of stimulus processing and detection, i.e., SEPs, we averaged spectral amplitudes within the alpha- (9–14 Hz) and beta band (20–30 Hz) for each participant and those time-frames that showed the peak significant difference between detected and rejected trials for averaged near-threshold stimulation conditions (i.e., NTH66% and STH). After normalizing to the individual condition means (Cousineau et al., 2005), these oscillatory amplitudes were added as additional predictors to the mentioned model and were allowed to interact with the P50 and N150 amplitude. Again, we used 6-fold cross-validation in order to identify the optimal tuning parameter for regularization of the logistic regression model. Regularized logistic regression was implemented with the "glmnet" package in R (Friedman et al., 2010).

As we find a difference in average stimulation intensities for the STH stimulation condition (reported later), the observed effects on prediction might be confounded by the physical stimulation intensity. Thus, we partialed out the shared variance of stimulus intensity and SEP amplitude to control for this potential bias and re-ran the forgoing analysis. For this, we normalized every NTH66 and STH stimulation intensity for detected and rejected trials relative to the individually maximum stimulation current (either detected or rejected trials) so that normalized intensity values were either one or less. These normalized intensities correlate moderately with P50 amplitude (0.22). The variance of the normalized intensities was then paritialed out from each neural marker that we used in the regression and ANOVA models (see next section) by calculating a linear regression for the neural marker on normalized stimulation intensity and storing the residuals of the individual model fits. These residuals were then taken as new predictors in the regularized regression analysis and dependent variables in the ANOVA.

2.4.5. Statistical analysis concerning the interaction of stimulation intensity and pulse detection for SEP and rolandic rhythm amplitudes

We tested the effect of stimulus detection and stimulation intensity on somatosensory electrophysiological response strength by calculating SEPs separately for detected and rejected trials. Average potentials were required to consist of, at least, seven trials per condition to assure reasonable noise reduction. The majority of participants (N = 22) had less than seven detected trials for stimulus intensities below NTH66%. Therefore, only NTH66% and STH trials were analyzed subsequently, and data of four additional participants had to be rejected for falling below this trial threshold in the remaining stimulation conditions, resulting in on average 25 (13 SD) and 68 (10 SD) detected and 64 (14 SD) and 19 (8 SD) rejected trials for NTH66% and STH stimulation intensities. P50 and N150 amplitudes of the remaining 32 participants were subjected to a 2 x 2 repeated measures ANOVA's with factors "detection" (stimulus detected vs. rejected) and "stimulus intensity" (STH vs. NTH66%). ANOVA statistics and bootstrapped confidence intervals (resampling of subject indices for each condition with 10,000 iterations) were computed with the ez-package developed by Mike Lawrence (Lawrence, 2013, version 4.2–2, https://github.com/mike-lawrence/ez). Effect sizes were quantified as generalized eta-squared (η_G^2, Bakeman, 2005).

We conducted similar repeated measures ANOVAs for the pre-stimulus alpha and beta amplitude on stimulus detection as for the SEP potentials with the factors "detection" and "stimulus intensity" to test a potential effect of covariates introduced by post-hoc condition sorting into detected and rejected trials. To be clear, any detection related effect through pre-stimulus oscillatory amplitude differences should be present for both stimulation intensities. If not, this could point to the confounding influence of another variable for which the experimental design does not control.

3. Results

3.1. Behavioral responses

Table 1 lists the mean intensity of electrical stimuli across all subjects for the six conditions, respectively.

Participant's sensitivity to single electrical current pulses increased, as expected, with the stimulation intensity from ADTH to STH (ADTH: $d' = 0.05$; $t(35) = 0.82$; $p = 0.21$; NTH33%: $d' = 0.48$; $t(35) = 5.81$; $p < 0.000001$; NTH66%: $d' = 1.53$; $t(35) = 16.87$; $p < 1.0*10\hat{}-15$; STH: $d' = 3.03$; $t(35) = 34.77$; $p < 1.0*10\hat{}-15$). Subthreshold stimulation trials, however, exerted d' values close to zero (Fig. 1; subTH-30%: $d' = -0.16$; subTH-15%: $d' = -0.19$; all $t(35)<-2.5$).

D-prime of ADTH intensities and below are not significantly higher than zero. This null-difference is, however, not proof of chance performance and therefore evidence for the Null hypothesis (NH) was evaluated against evidence for the alternative hypothesis of above chance performance by Bayes factor statistics (Rouder et al., 2009). As subthreshold intensities might suffer from oversampling compared to catch-trials, the z-transformation of low "yes"-response rates would artificially amplify any difference between both conditions concerning d' values. Thus, Bayes factors are calculated as paired one-sample one-sided test of the hit against false alarm rates and confirm chance performance with moderate to strong evidence in favor for the NH (FAR = 0.018; subTH-30%: HR = 0.018, $BF_{01} = 6.1$; subTH-15%: HR = 0.016, $BF_{01} = 10.8$). Widely different scaling of the JZS prior revealed that evidence for the null hypothesis, i.e., chance performance after subthreshold stimulation, outweighs evidence for the alternative for virtually all prior widths between 0.1 and 1.5 (Fig. 2 b-c, left). Evidence for the ADTH data is mixed: the posterior odds favor the alternative when the expected effect size is small (i.e., narrow prior, $r = 0.0757$) as compared to when the prior weights bigger effects more strongly (wide prior, Fig. 2 d, left). Sequential tests show that the Bayes Factor reliably favors the NH across different sample sizes.

To test further evidence for the NH, we calculated a Bayes factor meta-analysis (Rouder and Morey, 2011) based on the current detection rates of subthreshold stimulation intensities and a similar but independent psychophysics dataset published in Forschack et al. (2017). Accumulated evidence moderately to strongly favors chance performance for subthreshold stimulation magnitudes ($r = \sqrt{2}/2$, subTH-30%: $BF_{01} = 6.73$, subTH-15%: $BF_{01} = 12.18$). The Bayes factor for the comparison between d' values of stimulation magnitudes 85% against 70% of ADTH electrical current (JZS prior width $r = \sqrt{2}/2$) revealed that there is 8.14 times more evidence that perceptual sensitivity to the higher subthreshold intensity (subTH-15%) is equal to the lower intensity (subTH-30%) as compared to the alternative hypothesis.

3.2. SEP amplitudes and latencies change along the psychometric function

The grand-average SEP across all stimulation conditions over contralateral central electrode sites (Fig. 3) shows a positive and negative deflection that peaked at 52 ms (P50) and 142 ms (N150) after stimulus onset, respectively. Statistical comparison of the post-stimulus window (0–300 ms) against pre-stimulus baseline (−100 to 0 ms) via TFCE showed two lateralized cluster being significant for the P50 and a contralateral cluster of electrodes being significant for the N150. As our a-priori electrode selection for SEP analysis matched the result of the permutation test, we went on analyzing C4 for all further statistical tests concerning the SEP.

Imperceptible stimulation (*d*-prime around 0, both subTH-30%, and subTH-15%) elicited a P50 after stimulation, but no N150. In contrast, above threshold stimulation evoked both components (Fig. 4).

Generally, both P50 and N150 component peak amplitudes were largest for the highest and lowest for the smallest stimulation intensity, respectively. In Fig. 4, sample means for each condition are plotted together with within-subject 95%-confidence intervals, so that

Table 1
Average electrical current in milliampere (mA) for all stimulation conditions. For the relative intensities, stimulation magnitudes were normalized to ADTH. subTH = subthreshold, ADTH = absolute detection threshold, NTH = near threshold, STH = supra threshold, M = mean, SD = standard deviation.

Condition	subTH (−30%)	subTH (−15%)	ADTH	NTH 33%	NTH 66%	STH
M (mA)	1.12	1.35	1.59	2.01	2.42	2.84
SD (mA)	0.41	0.51	0.59	0.61	0.67	0.75
Range (mA)	0.47–2.03	0.52–2.5	0.66–2.91	0.91–3.39	1.11–3.87	1.24–4.35
Rel. Intensity	0.70	0.85	1	1.3	1.6	1.9

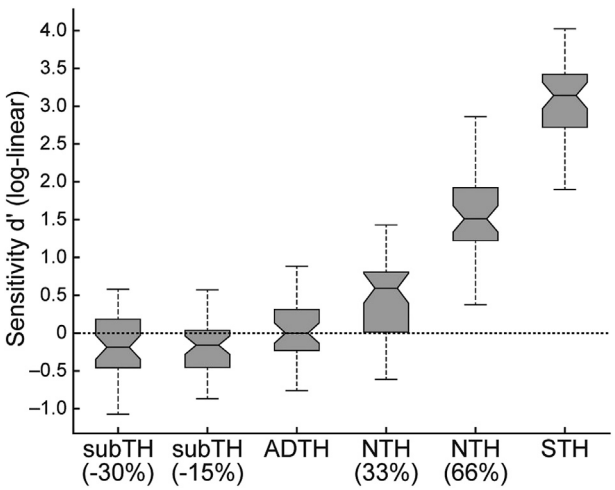

Fig. 1. Boxplots depict individually group-averaged d-prime values for the six different stimulation intensity categories showing that participants are zero sensitive to stimulation intensities below the individually adjusted absolute detection threshold (ADTH). Subthreshold (subTH) stimulation intensities were individually adjusted to 15% and 30% below ADTH. Near-threshold (NTH) intensities were tuned to 33% and 66% of the distance between ADTH and supra threshold (STH) intensity. Raw hit and false alarm rates were corrected according to Hautus (1995) to account for extreme values (i.e., no responses to target or catch trials). Notches indicate 95% confidence intervals.

significant differences are directly observable. Pairwise *t*-tests for all possible intensity pairs revealed significant P50 amplitude differences (fdr-corrected) from both subthreshold intensities to all above threshold intensities (all $t(35) < -3.1$, $p_{fdr} < 0.01$) but no difference was observed to the ADTH intensity (all $t(35) > -1.35$). ADTH P50 amplitude was significantly smaller than NTH33% and STH ($t(35) < -2.8$, $p_{fdr} < 0.02$), however, the amplitude difference to NTH66% was not significant ($t(35) = -1.85$. Both NTH33% and NTH66% P50 amplitudes were significantly smaller than P50 amplitude of STH (all $t(35) < -4$, $p_{fdr} < 0.001$). No statistical difference was observed between the P50 amplitudes of the subthreshold stimulation conditions (subTH-30%-subTH-15%: $t(35) = -0.77$, $p_{fdr} = 0.48$) and the near-threshold conditions (NTH33%-NTH66%: $t(35) = 0.36$, $p_{fdr} = 0.72$).

Estimates of N150 amplitudes of the subthreshold stimulation conditions were not different from zero and therefore significantly smaller than all other N150 amplitudes of the above threshold stimulation conditions (all $t(35) \geq 2.2$, $p_{fdr} \leq 0.04$, except for the subTH-30%-ADTH difference: $t(35) = 1.92$, $p_{fdr} = 0.08$). There was no significant difference between ADTH and NTH33%, as well as between NTH66% and STH N150 amplitudes (all $t(35) \leq 1.35$). All other above threshold stimulation conditions differed significantly in N150 amplitude (all $t(35) > 2.5$, $p_{fdr} < 0.03$).

In two previous studies (Forschack et al., 2017; Nierhaus et al., 2015), we noticed a P50 latency shift for subTH-15% compared to STH stimulation intensities but did not explicitly test this difference. Here, a direct test of the two conditions was not significant ($t(35) = 1.4$, $p = 0.17$). P50 of NTH33% stimulation intensitiy peaked significantly later than P50 of STH ($t(35) = 2.05$, $p = 0.048$). However, no test survived correction for multiple comparisons when all possible condition combinations were tested ($-1.5 < t(35) < 1.6$). N150 latencies were significantly different only for the peak latency comparison between ADTH and NTH66% ($t(35) > 2.97$, $p_{fdr} < 0.01$, all other: $-1.4 < t(35) < 1.9$).

The SEP waveforms of the different stimulation conditions are shown in Fig. 5. The post-hoc *t*-test of the averaged subTH waveform against baseline showed no significant components ($p_{fdr} \geq 0.05$).

3.3. Pre-stimulus rolandic rhythms predict stimulus detection

We assessed the overall effect of pre-stimulus alpha (9–14 Hz), and beta band (20–30 Hz) amplitudes on near-threshold stimulus detection by comparing the averaged STH and NTH66% stimulation conditions between detected and rejected stimuli at a contralateral central and an ipsilateral frontal electrode cluster. As depicted in Fig. 6, the difference in beta-band amplitude did not survive correction for multiple comparisons at a *p*-level of 0.01. However, according to Schubert et al. (2008), who found a frontal electrode cluster showing a significant beta-band amplitude difference around 200 ms preceding detected and rejected stimuli, we had a strong a priori hypothesis about where and when pre-stimulus beta-band amplitude differs with respect to stimulus onset. In fact, the frontal beta amplitude here was significantly larger 196 ms preceding detected stimuli (indicated as vertical line in Fig. 6a, upper-middle panel, $t(35) = 2.74$, $p < 0.01$, uncorrected) as compared to rejected stimuli. When testing it with a two-way repeated-measures ANOVA modeling the factors "detection" (detected vs rejected) and "time" (−400 to −100 ms) as indicated by none-overlapping confidence intervals of Fig. 6a (upper middle panel), the peak difference was still significant.

Furthermore, there is a pronounced alpha-band amplitude difference with alpha being lower for successively detected stimuli as compared to rejected stimuli that survive multiple comparison correction at $p < 0.01$ for a time range that extended from −336 to −232 ms relative to stimulus onset (lower middle part of Fig. 6). Topographic maps (right panels of Fig. 6) depict beta- and alpha-band scalp amplitude distributions for the time-frame with the smallest (uncorrected) *p*-values (indicated by the vertical line in the middle panels of Fig. 6).

3.4. N150 amplitude and pre-stimulus rolandic rhythms best explain stimulus detection

To assess whether additional neural features besides the amplitude of the respective SEP component are relevant for stimulus detection and rejection, we ran regularized binomial logistic regression models including both amplitude and latencies of the P50 and N150. The model with the smallest cross-validation error (CVE) only contains N150 amplitude as a regressor for stimulus detection and is accurate in 71% of the tested cases ($p < 0.001$, Fig. 7 top). Model complexity was reduced by shrinking the non-predictive coefficients (N150 latency as well as P50 amplitude and latency) to zero.

As we noticed in the previous analysis that pre-stimulus central alpha amplitude is higher during rejected stimulation than during detected stimulation and frontal beta amplitude is lower during rejected stimulation than during detected stimulation, we included both as a factor in the binomial regression model and allowed them to interact with the P50

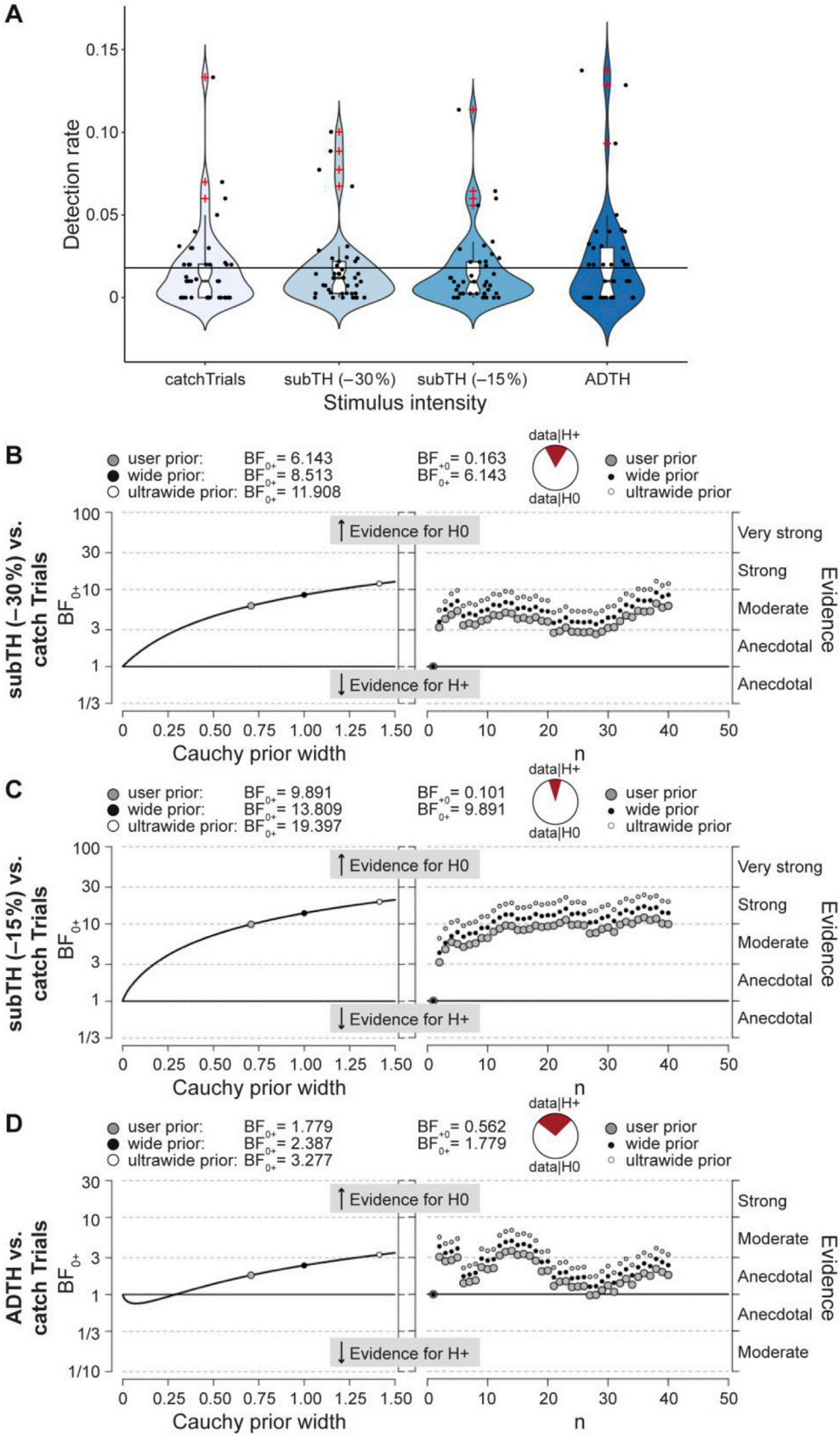

Fig. 2. A: Distributions of "yes"-response rates across all participants (dots) for those stimulation conditions for which d-prime values were not different from zero and the condition without stimulation (catch trials). The horizontal black line indicates the average false alarm rate. B–D: Bayes factor tests of hit rates of subTH-30% (B), subTH-15% (C) and ADTH (D) stimulus intensities against catch trial condition. Evidence for the null hypothesis (hit rates not different from false alarm rates) against the alternative hypothesis (hit rates greater than false alarm rates) along various Cauchy prior widths (left) is depicted as likelihood values higher than one. The grey filled circle marks the prior width used in the main analysis. On the right, sequential tests show evidence accumulation when adding single participants until the final sample size for three different prior widths. For subthreshold intensities, there is at least moderate evidence favoring the null hypothesis for all sample sizes.

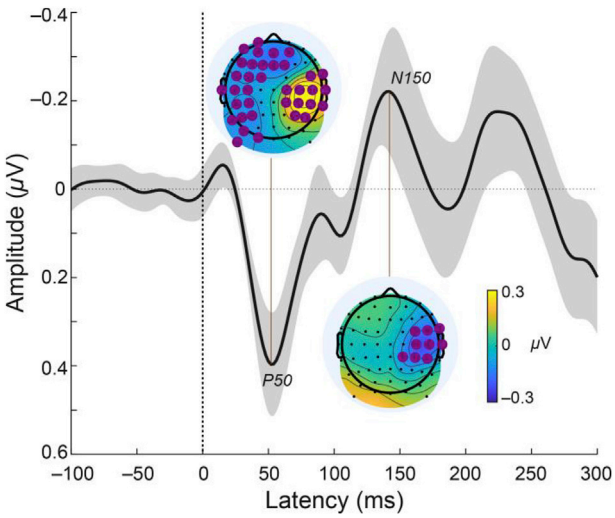

Fig. 3. Grand-average SEP waveform at C4 across all stimulation conditions together with topographic voltage maps for the P50 and N150, respectively. Shaded areas around the curve represent 95% confidence intervals of a running *t*-test for each time point against baseline. Purple colored electrodes in the topographic maps mark significant voltage changes compared to baseline at the indicated time point tested with a non-parametric permutation test (10,000 iterations) of the time window from 0 to 300 ms post-stimulus. Correction for multiple comparisons achieved by tfce (Mensen and Khatami, 2013).

and N150 amplitude. Interestingly, the model with the smallest CVE was accurate in 86% of the cases, contained alpha, and beta amplitude as main regressors and a beta - N150 amplitude interaction regressor (Fig. 7, bottom). That is, alpha amplitudes are inversely correlated with detection, whereas higher beta amplitudes are associated with detected stimuli. The interaction between N150 and beta amplitude signifies that a reduction in both measures goes in hand with rejected stimuli.

3.4. P50 amplitude is sensitive for stimulation intensity but not detection

To test the influence of stimulation intensity and detection on the early event-related potential, we modeled P50 and N150 amplitudes following detected and rejected NTH66% and STH stimulation intensities in a repeated measures design. The ANOVA revealed a significant main effect of stimulation intensity on P50 amplitude ($F(1,31) = 15.2$, $p = 0.0005$, $\eta_G^2 = 0.07$), but interestingly, neither the effect of detecting a successive stimulus ($F(1,31) = 0.57$) nor the interaction of intensity and detection was significant ($F(1,31) = 0.62$). In contrast, the detection of a successive stimulus showed a pronounced effect on the N150 amplitude (*detection*: $F(1,31) = 32.97$, $p = 0.00001$, $\eta_G^2 = 0.16$), but neither stimulation intensity ($F(1,31) = 3.83$, $p = 0.06$, $\eta_G^2 = 0.06$), nor the intensity-detection-interaction ($F(1,31) = 1.56$, $p = 0.22$, $\eta_G^2 = 0.006$) was significant. As depicted in Fig. 8a, all stimulation conditions resulted in a measurable P50. This is also true for the N150—except for rejected STH intensities—as indicated by the bootstrapped confidence intervals.

Average stimulation intensities across blocks differed significantly between detected and rejected trials for the STH stimulation condition ($M_{detected} = 2.84$ mA, $M_{rejected} = 2.79$ mA, $t(31) = 3.53$, $p = 0.0013$, maximum difference: 0.23 mA, i.e., two step sizes of the constant current stimulator, median difference: 0.04 mA), but not for NTH66% ($M_{detected} = 2.43$ mA, $M_{rejected} = 2.42$ mA, $t(31) = 1.26$, $p = 0.22$, maximum difference: 0.17 mA, median difference: 0.04 mA). However, after partialing out stimulation intensity variance from the SEP measures, P50 amplitude vanished for all factors (Fig. 8b, all $F(1,31) < 1.06$) but the effect of detection on N150 amplitude prevailed ($F(1,31) = 33.52$, $p < 0.00001$, $\eta_G^2 = 0.17$, all other $F(1,31) < 1.32$).

The experimental design required post-hoc condition labeling for the factor 'detection', which might introduce a collinearity between the detection of a stimulus and its stimulation intensity concerning the effect of pre-stimulus oscillatory amplitudes. Specifically, we suspected that if the nature of the alpha amplitude on detection is inhibitory, this might be easier to catch for relatively strong stimulation intensities. This is because missing a strong stimulus would then require relatively larger pre-stimulus alpha amplitudes, i.e., more functional inhibition. Fig. 9 and

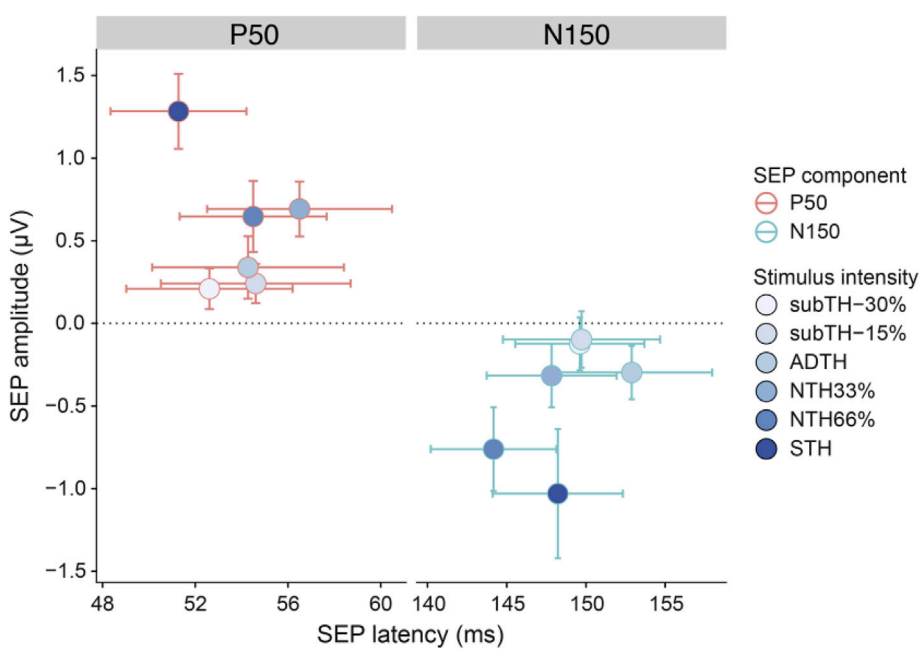

Fig. 4. Grand-averaged SEP amplitudes and latencies resulting from individual peak selection. Colored circles represent the sample average, for the P50 and N150, respectively. Circle filling color corresponds to the stimulation condition. Error bars based on within-subject error (i.e., between-subject variance removed, according to Morey, 2008), both for amplitude (vertical bars) and latency (horizontal bars) at 95% of statistical confidence.

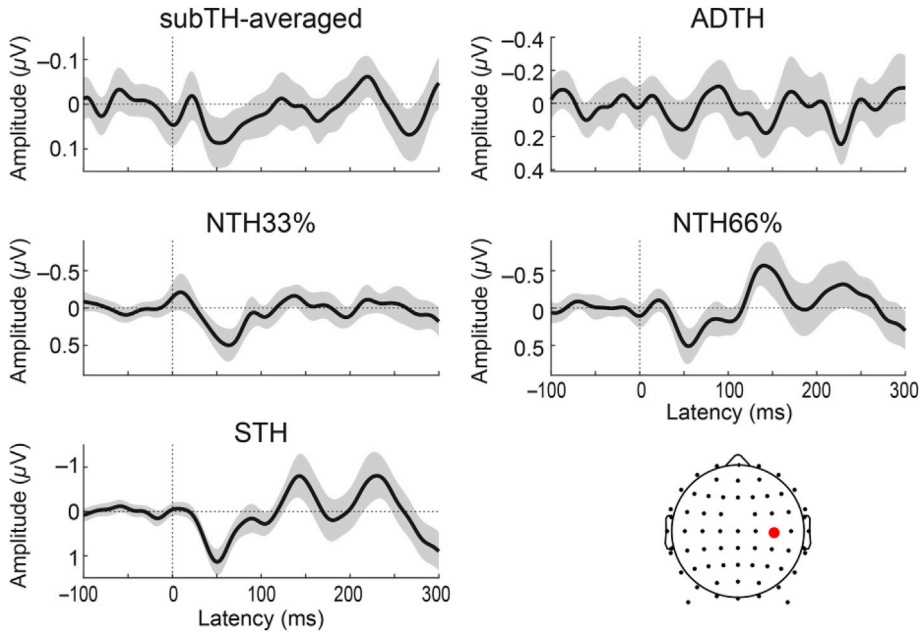

Fig. 5. Grand average SEP waveforms for all stimulation conditions at contralateral C4 electrode as indicated by the red dot in the bottom right plot. Shaded areas around the curve represent 95% confidence intervals of a running *t*-test for each time point against baseline. subTH-averaged: all trials with stimulus intensities below absolute detection threshold (ADTH). Note the different ordinate scaling.

the corresponding ANOVA seem to support this suspicion. There is a main effect of detection on pre-stimulus central alpha amplitude ($F(1,31) = 5.85$, $p = 0.02$, $\eta_G^2 = 0.08$; stimulation intensity: $F(1,31) = 1.33$, p = 0.26, $\eta_G^2 = 0.01$; intensity-detection-interaction: $F(1,31) = 1.38$, $p = 0.25$, $\eta_G^2 = 0.01$) and average pre-stimulus alpha amplitudes are significantly higher for rejected than detected STH trials only ($t(31) = -3.07$, p-value $= 0.004$). For pre-stimulus frontal beta amplitude, we observe a stimulus intensity main effect ($F(1,31) = 9.27$, $p = 0.005$, $\eta_G^2 = 0.05$; detection: $F(1,31) = 4.08$, $p = 0.052$, $\eta_G^2 = 0.05$, intensity-detection-interaction: $F(1,31) = 2.1$, $p = 0.16$, $\eta_G^2 = 0.03$) that is driven by a significant reduction of beta amplitude preceding rejected STH intensity compared to all other conditions (detected STH: $t(31) = -2.4$, $p = 0.02$; rejected NTH66%: $t(31) = -2.67$, $p = 0.01$; detected NTH66%: $t(31) = -2.88$, $p = 0.007$).

4. Discussion

We investigated, which early electrophysiological features are related to the encoding of stimulation intensity and the decoding of stimulus detectability in a two-response-classification-task for various stimulation intensities along the individual psychometric response function. Importantly, by including stimulation intensities below absolute detection threshold (ADTH), we quantified how measures of imperceptible stimulation (subthreshold) dissociate from stimulation above ADTH that may or may not be detected. For the subthreshold stimuli, the SEP exhibited only a P50 component, thereby replicating previous research (Forschack et al., 2017; Libet et al., 1967; Nierhaus et al., 2015; Ray et al., 1999). Despite this early cortical processing participants are clearly null sensitive for the subthreshold stimuli. P50 amplitude scaled with increasing stimulation intensities but was not predictive for detection; N150 is the earliest component reflecting stimulus detection. A model with lower pre-stimulus somatosensory alpha and higher frontal beta amplitudes together with an interaction of pre-stimulus frontal beta and the negative potential 150 ms after stimulus onset (N150) best explained somatosensory stimulus detection.

Investigations on perception without awareness require testing of the null-hypothesis (NH) that stimuli cannot be detected. In our experiment, Bayes Factors clearly supported chance performance of detection when subjects were stimulated below ADTH, i.e., false-positive responses upon null stimulation were equally likely. Nevertheless, these stimuli evoke the P50 component. In contrast, for stimulation above ADTH, participants show increasing perceptual sensitivity with stronger stimulation intensities and the largest P50 component after suprathreshold (STH) stimulation. Thus, the presence of the P50 does not provide sufficient evidence for perceptual awareness (Forschack et al., 2017; Nierhaus et al., 2015) but together with the absence of the N150 component dissociates processing of stimulation below ADTH from stimulation above it.

Above ADTH, stimulation evokes the N150 even for rejected near-threshold (NTH) stimuli, suggesting that mere presence of the N150 also does not provide sufficient evidence for detection. However, the N150 was not present for rejected stimuli at the highest intensity (STH). This might be a result of different trial numbers for detected and rejected stimulation conditions: STH-SEPs are based on the smallest number of rejected trials, thus SNR for these trials is poor, thereby reducing the likelihood of capturing a small potential. Another explanation would be that it is less likely to make a negative report ("rejected") after a relatively strong stimulation.

So far, we discussed the effect of perceptual sensitivity and detection on the *presence or absence* of the P50 and N150. However, sensitivity or detection may relate to the component's *amplitude difference* between detected and rejected stimulation trials. Despite being positively dependent, our results suggest two independent mechanisms for encoding stimulus intensity and detection within the event-related potential. First, P50 amplitudes scale to stimulus intensity but, second, only higher N150 amplitudes, i.e., a more negative potential, appeared to be predictive for detecting a given stimulus. Importantly, this finding shows that investigating the influence of perceptual awareness on early SEP amplitudes with near-threshold stimulus intensities (50% detection performance) requires the stimulation intensities to be fixed. Otherwise, the effects of stimulation intensity and perceptual reports are conflated concerning SEP amplitudes. The studies by Weisz et al. (2014) and Wühle and colleagues (2010) showed that ongoing staircase produces different stimulation intensities for detected and undetected (however, they did not analyze early SEP to these stimuli). In our study, we kept stimulation intensities constant for a given block; however, we adjusted these between blocks to account for

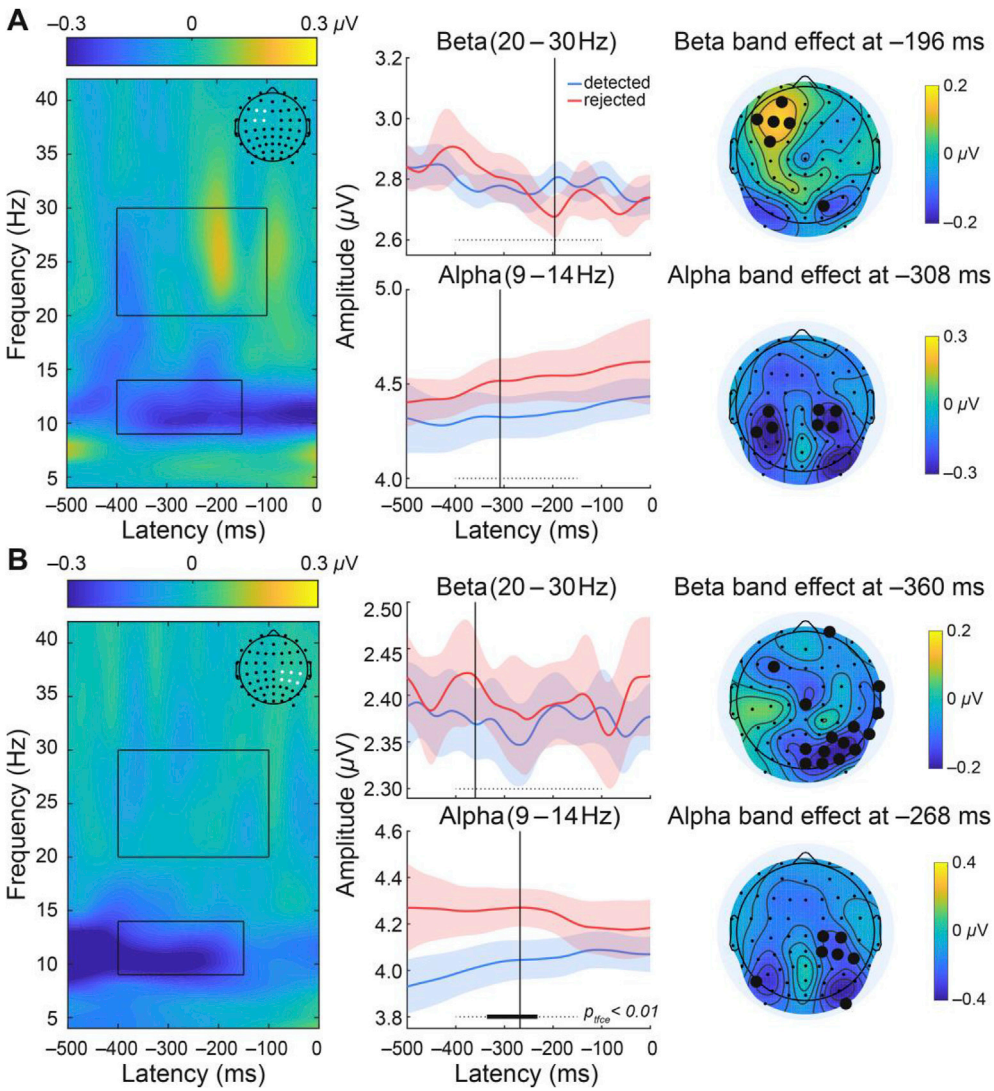

Fig. 6. Grand average pre-stimulus oscillatory amplitude effects on subsequent stimulus detection for an ipsilateral frontal (A) and contralateral central electrode cluster (B) and a time window of interest according to Schubert et al. (2008). Left panels: Time-frequency amplitude difference of averaged NTH66% and STH stimulation conditions at the averaged frontal (A) and central (B) electrode cluster, respectively, highlighted as white dots in the topographic map insets. Black boxes mark the a-priori defined time-frequency-windows for subsequent statistical analysis of alpha- and beta band responses, respectively. Middle panels: Grand average Alpha- and beta band pre-stimulus time courses preceding detected and rejected stimuli. Average values are plotted together with within-subject confidence intervals according to Cousineau et al. (2005) and Morey (2008) at a 95% confidence level. Horizontal dotted line indicates a paired *t*-test, thresholded at $p = 0.01$, and cluster-corrected for multiple comparisons with tfce (Mensen and Khatami, 2013). The bold line depicts the period with amplitude differences exceeding this threshold. Vertical lines indicate the amplitude difference showing the smallest p-value, subsequently used for representing the topographic changes across all electrodes. Right panels: Topographic amplitude difference at the most prominent time point (indicated by the vertical lines of the middle part of the figure) for both alpha- and beta band. Thick black electrodes showed a difference at an uncorrected *p*-level of 0.05. No test survived multiple comparisons correction.

threshold shifts. Although stimulation intensities differed slightly for the STH condition between detected and rejected trials (<0.1–0.2 mA, current step size of the DS7: 0.1 mA), there was no significant difference regarding the P50 amplitude, which is sensitive to stimulation intensity (see above). Stimulation intensities did not differ for the detected and rejected trials of the NTH66% condition, but N150 nevertheless was more pronounced (more negative) for detected trials. These results were still confirmed when accounting for physical stimulation intensities between blocks by partialing out stimulation current variances. Taken together, STH electrical current differences did not affect SEP amplitudes concerning the detectability of the stimuli.

Past research, however, found the P50 amplitude indicative for stimulus detectability. Eimer et al. (2002) studied an extinction patient suffering from a right-hemispheric stroke. The patient was able to recognize left unilateral stimuli to the index finger; however, contralesional stimuli were missed—i.e., extinguished—on 75% of the trials when concurrently presented together with a stimulus at the right index finger. Contralateral SEP responses to these extinguished left stimuli contained a P50 and N110, which were not present at the same sites during unilateral right stimulation but were numerically, however not statistically, smaller as compared to (felt) unilateral left stimulation. Furthermore, unilateral contralesional left stimulation resulted in smaller components over the damaged hemisphere as compared to left hemisphere responses found after unilateral right stimulation. These results led to the hypothesis that extinction may arise from attenuation rather than the absence of early event-related components. Interestingly, components over the damaged hemisphere on bilateral extinguished trials were not different from felt unilateral left stimulation, suggesting that concurrent right tactile events might trigger competitive mechanisms that influence early tactile processing. Modulations of the P50 amplitude affecting perceptual awareness, therefore, seem to be less pronounced when stimuli are presented in isolation (Eimer et al., 2002), as it is the case for our study.

In our previous studies (Nierhaus et al., 2015; Forschack et al., 2017), P50 to the suprathreshold stimulation intensity peaked roughly 10 ms earlier than to the subthreshold intensity. At the physiological level, this latency effect might indicate a shifted excitation-inhibition-balance towards a dominant rapid activation of principal excitatory neurons (Isaacson and Scanziani, 2011; Nierhaus et al., 2015). On the cognitive level, one might argue that STH stimuli trigger exogenous attention more reliably than weaker stimulation intensities. Thus, SEPs evoked by attended stimuli show a shorter latency than those evoked by unattended stimuli (see Spence and Parise (2010) for an overview of "Titchener's law of prior entry"). Here, however, we could only find an uncorrected significant latency shift for the STH versus NTH33% intensity and SEP latencies were not predictive for stimulus detection in the regression models. Thus, SEP latency shifts do not seem to be indicative of stimulus intensity or stimulus detectability.

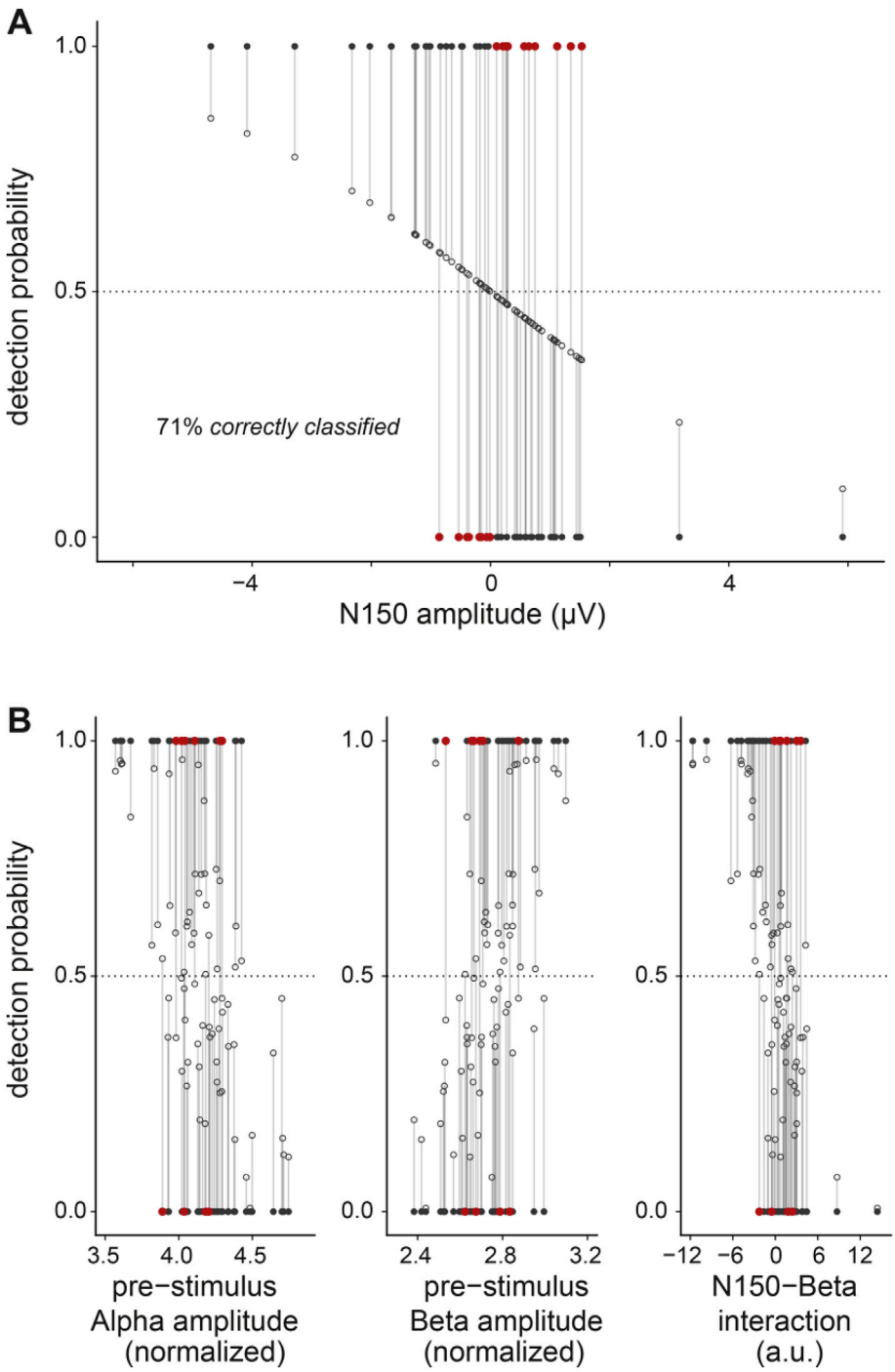

Fig. 7. Detection probability predicted by the lasso regularized binomial logistic regression showing the smallest cross-validation error (empty circles) together with the actual subject-level response data (filled circles). A: Response prediction when only SEP features were included as predictors, i.e. P50 and N150 amplitude and latency. Winning model only contains N150 amplitude as significant regressor for behavioral responses. Grey lines represent the model error, the shorter the better. Black circles correspond to correctly, red circles to incorrectly classified responses. B: Winning model when including pre-stimulus central alpha and frontal beta amplitudes averaged at 268 ms and 196 ms, respectively, preceding detected and rejected stimuli. This model correctly classifies 86% of the cases. Between subject-variance was removed for alpha and beta band amplitude values in order to center them along the behavioral response differences.

Regarding the role of the N150 as a marker of stimulus detection, our results are in line with previous research (Auksztulewicz et al., 2012; Cauller and Kulics, 1991; Schubert et al., 2006; Zhang and Ding, 2009). However, none of these studies, including our own, provide evidence for a proper neural correlate of consciousness (NCC, Aru et al., 2012), because task paradigms will necessarily conflate perceptual awareness with decisional processes (but see Schröder et al., 2019). It has been pointed out that an NCC proper must not cease when participants passively perceive suprathreshold stimuli without any task (Hillyard et al., 1971; Squires et al., 1973; Verleger, 2010). In Nierhaus et al. (2015), we found the N150 during electrical finger stimulation well above ADTH while participants had no task. This provides initial suggestive evidence for the N150 resembling an NCC proper (Aru et al., 2012). Future studies should include a passive and an active condition within one experiment while sampling intensities close to NTH50% threshold. To re-evaluate the effect of the P50 amplitude on perceptual awareness, these studies might present bilateral tactile stimuli that trigger competitive early-stage processes and hence could increase the influence of the P50 amplitude on the perceptual fate of near-threshold stimuli (Eimer et al., 2002).

Finally, the current study replicates a large body of research showing that pre-stimulus alpha amplitude is predictive for the detectability of upcoming events (Chaumon and Busch, 2014; Craddock et al., 2017; Iemi et al., 2017; Limbach and Corballis, 2016; Linkenkaer-Hansen et al., 2004; Ruhnau et al., 2014; Schubert et al., 2008; Weisz et al., 2014; Zhang and Ding, 2009). Like these studies, we found that higher pre-stimulus alpha

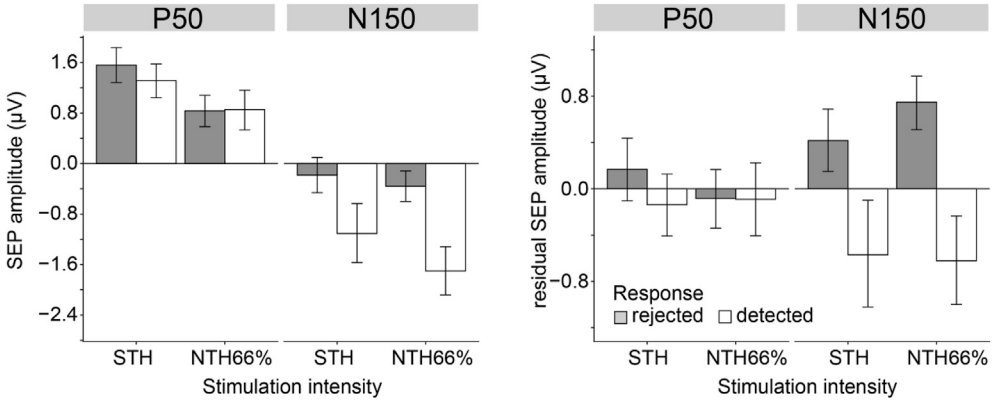

Fig. 8. Left: Grand mean P50 and N150 amplitudes for the strongest stimulation intensities (NTH66% and STH) and relative to the behavioral response (white bars = detected; grey bars = undetected stimuli). Right: The main effect of stimulation intensity on P50 amplitude disappears when stimulus intensity variance is partialed out, however, the main effect of detection on the N150 amplitude remains. Bootstrapped 95% confidence intervals were obtained by shuffling condition labels across participants 10,000 times and indicate presence of the component within the specific condition when not overlapping with the line at zero (i.e., amplitude is significant from zero).

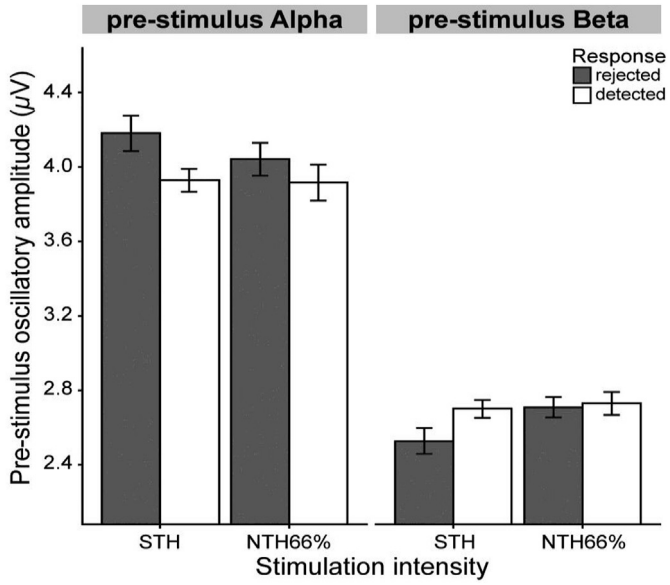

Fig. 9. Grand mean pre-stimulus alpha and beta amplitudes for the two strongest stimulation intensities (NTH66% and STH) plotted for the factors stimulation intensity and behavioral response (white bars = detected; grey bars = undetected stimuli). Bootstrapped 95% confidence intervals were obtained by shuffling condition labels across participants 10,000 times.

went along with negative behavioral responses. Additionally, higher frontal beta amplitudes preceded detected trials. This is in contrast to findings where smaller beta amplitudes paralleled decreased alpha-band activity that either indicated sensorimotor processing, e.g., in motor preparation (Pfurtscheller and Lopes da Silva, 1999), prevented intrusions from task-irrelevant competing stimuli (Schubert et al., 2008), or reflected anticipatory activity (Bauer et al., 2006; Ede et al., 2014; Schubert et al., 2008; but see Haegens et al. (2012) for a concomitant increase of alpha in subjects awaiting stimulation). Whereas a higher central alpha amplitude preceding *rejected* stimulation seems consistent with its presumed inhibitory function, a higher frontal beta amplitude preceding *detected* stimulation might indicate an endogenous content (re)activation that supports the transition from latent to active task representations thereby forming functional neural ensembles in the service of the current demands (Spitzer and Haegens, 2017). It may appear surprising that the pre-stimulus oscillatory amplitude effect on detection is only present preceding the strongest stimuli but not the second strongest. However, this might be an effect of the post-hoc condition split according to detected and rejected stimuli: a high pre-stimulus (inhibitory) alpha amplitude might be required to miss a strong stimulus; likewise, an improperly formed neural ensemble reflected by (too) small content-specific frontal beta amplitudes may turn a strong stimulus undetectable.

In conclusion, stimulus detection might emerge from a serial process where early intensity encoding precedes stimulus recognition. While the earliest evoked potential related to stimulus detection (N150) was absent during completely imperceptible stimulation, thus emphasizing its involvement in stimulus recognition, the preceding P50 was cleary measurable during all stimulus conditions. Besides the neural representation of stimulus intensity, the P50 did not predict stimulus recognition of detectable stimuli. Furthermore, alpha- and beta amplitude dynamics seem to render upcoming stimulation being reportable or not, but probably support different aspects of the stimulus recognition process. Future studies are required to disentangle the contribution of those frequency bands to the emergence of perceptual awareness.

Author contributions

N.F., T.N., M.M.M., and A.V. designed research; N.F. performed research; N.F., T.N. contributed unpublished reagents/analytic tools; N.F. analyzed data; N.F., T.N., M.M.M., and A.V. wrote and revised the paper.

Declaration of competing interest

The authors declare no competing financial interest.

Acknowledgements

This study was funded by Max Planck Society and the Deutsche Forschungsgemeinschaft (MU 972/26–1). We thank Sylvia Stasch for the recruitment of participants, her help with data recording, and Heike Schmidt-Duderstedt and Kerstin Flake for rendering figures for publication.

References

Anderson, K.L., Ding, M., 2011. Attentional modulation of the somatosensory mu rhythm. Neuroscience 180, 165–180.
Aru, J., Bachmann, T., Singer, W., Melloni, L., 2012. Distilling the neural correlates of consciousness. Neurosci. Biobehav. Rev. 36, 737–746.
Auksztulewicz, R., Blankenburg, F., 2013. Subjective rating of weak tactile stimuli is parametrically encoded in event-related potentials. J. Neurosci. 33, 11878–11887.
Auksztulewicz, R., Spitzer, B., Blankenburg, F., 2012. Recurrent neural processing and somatosensory awareness. J. Neurosci. 32, 799–805.
Bakeman, R., 2005. Recommended effect size statistics for repeated measures designs. Behav. Res. Methods 37, 379–384.
Bauer, M., Oostenveld, R., Peeters, M., Fries, P., 2006. Tactile spatial attention enhances gamma-band Activity in somatosensory cortex and reduces low-frequency activity in parieto-occipital areas. J. Neurosci. 26, 490–501.
Baumgarten, T.J., Schnitzler, A., Lange, J., 2016. Prestimulus alpha power influences tactile temporal perceptual discrimination and confidence in decisions. Cerebr. Cortex 26, 891–903.
Baumgarten, T.J., Königs, S., Schnitzler, A., Lange, J., 2017. Subliminal stimuli modulate somatosensory perception rhythmically and provide evidence for discrete perception. Sci. Rep. 7, 43937.
Benjamini, Y., Hochberg, Y., 1995. Controlling the false discovery rate: a practical and powerful approach to multiple testing. J. R. Stat. Soc. Ser. B Methodol. 57, 289–300.

Bernat, E., Bunce, S., Shevrin, H., 2001a. Event-related brain potentials differentiate positive and negative mood adjectives during both supraliminal and subliminal visual processing. Int. J. Psychophysiol. 42, 11–34.

Bernat, E., Shevrin, H., Snodgrass, M., 2001b. Subliminal visual oddball stimuli evoke a P300 component. Clin. Neurophysiol. 112, 159–171.

Bigdely-Shamlo, N., Mullen, T., Kothe, C., Su, K.-M., Robbins, K.A., 2015. The PREP pipeline: standardized preprocessing for large-scale EEG analysis. Front. Neuroinf. 9.

Blankenburg, F., Taskin, B., Ruben, J., Moosmann, M., Ritter, P., Curio, G., Villringer, A., 2003. Imperceptible stimuli and sensory processing impediment. Science 299, 1864–1864.

Cauller, L.J., Kulics, A.T., 1991. The neural basis of the behaviorally relevant N1 component of the somatosensory-evoked potential in SI cortex of awake monkeys: evidence that backward cortical projections signal conscious touch sensation. Exp. Brain Res. 84, 607–619.

Chaumon, M., Busch, N.A., 2014. Prestimulus neural oscillations inhibit visual perception via modulation of response gain. J. Cognit. Neurosci. 26, 2514–2529.

Chaumon, M., Bishop, D.V.M., Busch, N.A., 2015. A practical guide to the selection of independent components of the electroencephalogram for artifact correction. J. Neurosci. Methods 250, 47–63.

Cousineau, D., Montréal, U.D., Paradis, T.T.D., For, D.C., 2005. Confidence intervals in within-subject designs: a simpler solution to Loftus and Masson's method. Tutorial in Quantitative Methods for Psychology.

Craddock, M., Poliakoff, E., El-deredy, W., Klepousniotou, E., Lloyd, D.M., 2017. Pre-stimulus alpha oscillations over somatosensory cortex predict tactile misperceptions. Neuropsychologia 96, 9–18.

Delorme, A., Makeig, S., 2004. EEGLAB: an open source toolbox for analysis of single-trial EEG dynamics including independent component analysis. J. Neurosci. Methods 134, 9–21.

Delorme, A., Sejnowski, T., Makeig, S., 2007. Enhanced detection of artifacts in EEG data using higher-order statistics and independent component analysis. Neuroimage 34, 1443–1449.

Delorme, A., Palmer, J., Onton, J., Oostenveld, R., Makeig, S., 2012. Independent EEG sources are dipolar. PloS One 7, e30135.

Ede, F. van, Lange, F.P. de, Maris, E., 2014. Anticipation increases tactile stimulus processing in the ipsilateral primary somatosensory cortex. Cerebr. Cortex 24, 2562–2571.

Eimer, M., Maravita, A., Van Velzen, J., Husain, M., Driver, J., 2002. The electrophysiology of tactile extinction: ERP correlates of unconscious somatosensory processing. Neuropsychologia 40, 2438–2447.

Faul, F., Erdfelder, E., Lang, A.-G., Buchner, A., 2007. G*Power 3: a flexible statistical power analysis program for the social, behavioral, and biomedical sciences. Behav. Res. Methods 39, 175–191.

Ferrè, E.R., Sahani, M., Haggard, P., 2016. Subliminal stimulation and somatosensory signal detection. Acta Psychol. 170, 103–111.

Forschack, N., Nierhaus, T., Müller, M.M., Villringer, A., 2017. Alpha-band brain oscillations shape the processing of perceptible as well as imperceptible somatosensory stimuli during selective attention. J. Neurosci. 37, 6983–6994.

Frey, J.N., Ruhnau, P., Leske, S., Siegel, M., Braun, C., Weisz, N., 2016. The tactile window to consciousness is characterized by frequency-specific integration and segregation of the primary somatosensory cortex. Sci. Rep. 6, 20805.

Friedman, J., Hastie, T., Tibshirani, R., 2010. Regularization paths for generalized linear models via coordinate descent | friedman | journal of statistical software. J. Stat. Software 33.

Genovese, C.R., Lazar, N.A., Nichols, T., 2002. Thresholding of statistical maps in functional neuroimaging using the false discovery rate. Neuroimage 15, 870–878.

Green, D.M., Swets, J.A., 1966. Signal Detection Theory and Psychophysics. Wiley, New York.

Haegens, S., Luther, L., Jensen, O., 2012. Somatosensory anticipatory alpha activity increases to suppress distracting input. J. Cognit. Neurosci. 24, 677–685.

Hillyard, S.A., Squires, K.C., Bauer, J.W., Lindsay, P.H., 1971. Evoked potential correlates of auditory signal detection. Science 172, 1357–1360.

Iemi, L., Chaumon, M., Crouzet, S.M., Busch, N.A., 2017. Spontaneous neural oscillations bias perception by modulating baseline excitability. J. Neurosci. 37, 807–819.

Iliopoulos, F., Nierhaus, T., Villringer, A., 2014. Electrical noise modulates perception of electrical pulses in humans: sensation enhancement via stochastic resonance. J. Neurophysiol. 111, 1238–1248.

Isaacson, J.S., Scanziani, M., 2011. How inhibition shapes cortical activity. Neuron 72, 231–243.

James, G., Witten, D., Hastie, T., Tibshirani, R., 2015. An Introduction to Statistical Learning - with Applications in R. Springer, New York.

JASP Team, 2018. JASP (Version 0.8.6)[Computer Software].

Kingdom, F.A.A., Prins, N., 2009. Psychophysics: a Practical Introduction. Acad. Press.

Klostermann, F., Wahl, M., Schomann, J., Kupsch, A., Curio, G., Marzinzik, F., 2009. Thalamo-cortical processing of near-threshold somatosensory stimuli in humans. Eur. J. Neurosci. 30, 1815–1822.

Lawrence, M.A., 2013. Ez: Easy Analysis and Visualization of Factorial Experiments.

Lee, M.D., Wagenmakers, E.-J., 2013. Bayesian Cognitive Modeling: A Practical Course. Cambridge University Press, Cambridge.

Li, Y., Ma, Z., Lu, W., Li, Y., 2006. Automatic removal of the eye blink artifact from EEG using an ICA-based template matching approach. Physiol. Meas. 27, 425.

Libet, B., Alberts, W.W., Wright, E.W., Feinstein, B., 1967. Responses of human somatosensory cortex to stimuli below threshold for conscious sensation. Science 158, 1597–1600.

Limbach, K., Corballis, P.M., 2016. Prestimulus alpha power influences response criterion in a detection task. Psychophysiology 53, 1154–1164.

Linkenkaer-Hansen, K., Nikulin, V.V., Palva, S., Ilmoniemi, R.J., Palva, J.M., 2004. Prestimulus oscillations enhance psychophysical performance in humans. J. Neurosci. 24, 10186–10190.

Loftus, G.R., Masson, M.E.J., 1994. Using confidence intervals in within-subject designs. Psychon. Bull. Rev. 1, 476–490.

Macmillan, N.A., Creelman, C.D., 2004. Detection Theory: A User's Guide. Psychology Press, Mahwah, N.J.

Mensen, A., Khatami, R., 2013. Advanced EEG analysis using threshold-free cluster-enhancement and non-parametric statistics. Neuroimage 67, 111–118.

Merikle, P.M., Daneman, M., 1998. Psychological investigations of unconscious perception. J. Conscious. Stud. 5, 5–18.

Morey, R.D., 2008. Confidence intervals from normalized data: a correction to Cousineau (2005). Tutor. Quant. Methods Psychol. 4, 61–64.

Mullen, T., 2012. NITRC: CleanLine: Tool/Resource Info.

Nierhaus, T., Forschack, N., Piper, S.K., Holtze, S., Krause, T., Taskin, B., Long, X., Stelzer, J., Margulies, D.S., Steinbrink, J., et al., 2015. Imperceptible somatosensory stimulation alters sensorimotor background rhythm and connectivity. J. Neurosci. 35, 5917–5925.

Oldfield, R.C., 1971. The assessment and analysis of handedness: the Edinburgh inventory. Neuropsychologia 9, 97–113.

Oostenveld, R., Praamstra, P., 2001. The five percent electrode system for high-resolution EEG and ERP measurements. Clin. Neurophysiol. 112, 713–719.

Palmer, J.A., Kreutz-Delgado, K., Makeig, S., 2011. AMICA: an Adaptive Mixture of Independent Component Analyzers with Shared Components.

Palva, S., Linkenkaer-Hansen, K., Näätänen, R., Palva, J.M., 2005. Early neural correlates of conscious somatosensory perception. J. Neurosci. 25, 5248–5258.

Pfurtscheller, G., Lopes da Silva, F.H., 1999. Event-related EEG/MEG synchronization and desynchronization: basic principles. Clin. Neurophysiol. 110, 1842–1857.

R Core Team, 2014. R: A Language and Environment for Statistical Computing. R Foundation for Statistical Computing, Vienna, Austria.

Ray, P.G., Meador, K.J., Smith, J.R., Wheless, J.W., Sittenfeld, M., Clifton, G.L., 1999. Physiology of perception: cortical stimulation and recording in humans. Neurology 52, 1044–1049.

Rouder, J.N., Morey, R.D., 2011. A Bayes factor meta-analysis of Bem's ESP claim. Psychon. Bull. Rev. 18, 682–689.

Rouder, J.N., Speckman, P.L., Sun, D., Morey, R.D., Iverson, G., 2009. Bayesian t tests for accepting and rejecting the null hypothesis. Psychon. Bull. Rev. 16, 225–237.

RStudio Team, 2012. RStudio: Integrated Development Environment for R. RStudio, Boston, MA.

Ruhnau, P., Hauswald, A., Weisz, N., 2014. Investigating ongoing brain oscillations and their influence on conscious perception – network states and the window to consciousness. Conscious. Res. 5, 1230.

Schröder, P., Schmidt, T.T., Blankenburg, F., 2019. Neural basis of somatosensory target detection independent of uncertainty, relevance, and reports. ELife 8, e43410.

Schubert, R., Blankenburg, F., Lemm, S., Villringer, A., Curio, G., 2006. Now you feel it—now you don't: ERP correlates of somatosensory awareness. Psychophysiology 43, 31–40.

Schubert, R., Haufe, S., Blankenburg, F., Villringer, A., Curio, G., 2008. Now you'll feel it, now you won't: EEG rhythms predict the effectiveness of perceptual masking. J. Cognit. Neurosci. 21, 2407–2419.

Shevrin, H., 2001. Event-related markers of unconscious processes. Int. J. Psychophysiol. 42, 209–218.

Shevrin, H., Fritzler, D.E., 1968. Visual evoked response correlates of unconscious mental processes. Science 161, 295–298.

Smith, S.M., Nichols, T.E., 2009. Threshold-free cluster enhancement: addressing problems of smoothing, threshold dependence and localisation in cluster inference. Neuroimage 44, 83–98.

Spence, C., Parise, C., 2010. Prior-entry: a review. Conscious. Cognition 19, 364–379.

Spitzer, B., Haegens, S., 2017. Beyond the status quo: a role for beta oscillations in endogenous content (Re)activation. ENeuro 4. ENEURO.0170-17.2017.

Squires, K.C., Hillyard, S.A., Lindsay, P.H., 1973. Vertex potentials evoked during auditory signal detection: relation to decision criteria. Percept. Psychophys. 14, 265–272.

Swets, J.A., 1961. Is there a sensory threshold? Science 134, 168–177.

Swets, J.A., 1964. Signal Detection and Recognition by Human Observers. Wiley, New York.

Taskin, B., Holtze, S., Krause, T., Villringer, A., 2008. Inhibitory impact of subliminal electrical finger stimulation on SI representation and perceptual sensitivity of an adjacent finger. Neuroimage 39, 1307–1313.

Verleger, R., 2010. Markers of awareness? EEG potentials evoked by faint and masked events, with special reference to the "attentional blink. In: Czigler, I., Winkler, I. (Eds.), In Unconscious Memory Representations in Perception: Processes and Mechanisms in the Brain. John Benjamins Publishing Company, Amsterdam/ Philadelphia.

Weisz, N., Wühle, A., Monittola, G., Demarchi, G., Frey, J., Popov, T., Braun, C., 2014. Prestimulus oscillatory power and connectivity patterns predispose conscious somatosensory perception. Proc. Natl. Acad. Sci. Unit. States Am. 111, E417–E425.

Widmann, A., Schröger, E., Maess, B., 2015. Digital filter design for electrophysiological data – a practical approach. J. Neurosci. Methods 250, 34–46.

Wühle, A., Mertiens, L., Rüter, J., Ostwald, D., Braun, C., 2010. Cortical processing of near-threshold tactile stimuli: An MEG study. Psychophysiology 47 (3), 523–534. https://doi.org/10.1111/j.1469-8986.2010.00964.x.

Zhang, Y., Ding, M., 2009. Detection of a weak somatosensory stimulus: role of the prestimulus mu rhythm and its top–down modulation. J. Cognit. Neurosci. 22, 307–322.